Not to be cited without prior reference to the authors

International Council for the Exploration of the Sea
ICES CM 2005/U:06

Acoustic Techniques for Three-dimensional Characterization and Classification of the Pelagic Ecosystem

Characterizing the spatial distribution of a semi-demersal gadoid

Julian M. Burgos and John K. Horne

University of Washington School of Aquatic and Fishery Science
Fisheries Acoustics Research Lab
Box 355020
Seattle, WA 98195-5020
USA
jmburgos@u.washington.edu, jhorne@u.washington.edu

Abstract

High-resolution, two-dimensional measurements of density are collected routinely during echo-integration trawl surveys. Echo-trace classification (ETC), the detection of aggregations within echograms, is used to describe and analyze spatial distributions of pelagic organisms. This approach is appropriate for species that form well-defined schools, but is limited when used for species that form demersal layers or diffuse pelagic shoals. As an alternative to ETC metrics, we used landscape indices to quantify and characterize spatial heterogeneity walleye pollock (*Theragra chalcogramma*) density distributions. Survey transects were divided into segments of equal length and a series of landscape metrics were calculated to measure occupancy, fragmentation, acoustic density structure, and vertical distribution. Ordination and classification techniques were used to examine relationships among metrics and to develop a classification typology for spatial patterns. The resulting classification consisted of six echogram types. Visual inspection revealed that spatial patterns of segments assigned to each type were consistent, but considerable overlap existed among types. Spatial analysis revealed that types were spatially autocorrelated and that the location among types within the survey area differed.

Keywords: Aggregations, echo-trace classification, landscape indices, spatial pattern, walleye pollock.

Introduction

Acoustic data are collected to estimate the abundance of marine organism populations (Misund, 1997). During echo-integration-trawl surveys, spatial and temporal data are collected at a high resolution (e.g. 10 m vertical and 0.2 m. horizontal resolution) but when used to estimate biomass, data are integrated through the water column and binned horizontally at coarser scales (i.e. 0.5 nm). Data collected during these surveys also can provide information on the distribution of marine organisms (ICES 2000). A methodology commonly used to extract this information from acoustic data is echo-trace classification (ETC, Reid et al., 2000). Echo-trace classification consists of displaying acoustic data in echograms and using image-processing algorithms to detect aggregations of the species of interest. The algorithms calculate quantitative descriptors from each detected aggregation, including size, total acoustic density, and location in the water column. The description of aggregations obtained through echo-trace classification has been used to study processes in marine systems including shoal formation (Rose et al., 1995), predator-prey interactions (Vabø and Nøttestad, 1997), and vertical migrations (Gauthier and Rose, 2002).

Echo-trace classification may not be appropriate to characterize all spatial patterns observed in acoustic data. Algorithms used in echo-trace classification require input parameters that define minimum size, minimum density and minimum separation from other aggregations. Boundaries are set around groups of adjacent pixels that satisfy criteria defined by input parameters. But many marine organisms do not form clearly delimited aggregations. For example, gadoids form diffuse pelagic layers and continuous benthic layers or ‘carpets’ that lack well-defined edges (Fig. 1). These structures are not amenable to analysis through echo-trace classification because results are highly sensitive to input parameter values used by detection algorithms (Burgos and Horne, in preparation). Reid et al. (2000) suggested that the presence of these structures should be evaluated using visual inspection of elementary sampling distance units (ESDU) or echogram sections of equal length, but provided no recommendations on how to quantify their spatial pattern.

In one attempt to characterize spatial patterns of structures lacking well-defined edges, Bertrand et al. (2002) combined visual inspection of echograms with a set of metrics calculated for sections of echograms of equal length. Spatial aggregation categories included sound-scattering layer, nucleus in scattering layer, large aggregated structures, stick-shaped structures, and small aggregates. Metrics calculated in each echogram section included total acoustic density and percentage of cells with non-zero values. This approach enables the quantification of structures lacking well-defined edges. A limitation of this visual method is that classification of echotraces is somewhat subjective and can be time consuming. An extension of this approach would expand the number and types of aggregation metrics, and to obtain an objective (i.e. numerical) classification method.

In recent years, landscape ecology researchers have proposed a large number of metrics that measure spatial heterogeneity of categorical raster maps (e.g. McGarigal and Marks, 1995). In most cases, information on the spatial composition of the landscape (i.e. a region of interest) is displayed in raster maps, where each pixel is assigned to a category of landscape elements. This approach detects homogeneous regions (Gustafson, 1998) and calculates indices that quantify spatial heterogeneity including composition (i.e. number and proportion of patch types) and spatial configuration (i.e. size, shape, and location of patches and interspersion among patch types). In most cases, these metrics have been used to describe spatial heterogeneity of landscapes at relatively large scales (~100 km, e.g. Schumaker, 1996), although in limited cases have been used to describe small-scale spatial patterns in benthic communities (~1 m, e.g. Teixidó et al., 2002). The representation of acoustically-detected fish distributions in an echogram is analogous to a raster map. Landscape metrics may be a useful technique to characterize spatial heterogeneity of aquatic organisms at over a range of scales extending from approximately 20 m to 2000 m.

In this paper we develop methods to quantify and classify spatial patterns of acoustic scatterers, using a combination of landscape indices and additional metrics appropriate for acoustic data. We divided each echogram into a series of segments of equal length and calculated a series of metrics to describe the spatial distribution of acoustic density in each segment. We utilized ordination and cluster techniques to analyze the relationship among metrics and to classify echogram segment in a reduced number of typologies. Walleye pollock (*Theragra chalcogramma*, Gadidae) in the Bering Sea were used as the test species as it forms a diverse array of spatial distribution patterns, is an important species in the pelagic and semi-demersal ecosystems of the North Pacific and Bering Sea, and it sustains a large commercial fishery.

Methods

1. Data

The acoustic data used in this study were collected by the NOAA Alaska Fishery Science Center (AFSC) during two echo-integration trawl surveys in the eastern Bering Sea to obtain biomass estimates of walleye pollock. Surveys were conducted between February and March (winter survey, Fig. 2) and between June and August (summer survey, Fig. 3) of the year 2000. For this study we 5132 nautical miles (nm) of summer survey data divided into 25 transects. From the winter survey we used eight transects, totaling 375 nm. Acoustic data were collected using a Simrad EK500 echosounder, operating at a frequency of 38 kHz and a ping rate of 1 sec^{-1}, with a beam angle of 7^{o} (Honkalehto et al., 2002). Personnel of the AFSC analyzed the data using minimum threshold of –70dB and classifying the acoustic returns as walleye pollock or other species.

Data were imported into Echoview V. 3.10 (Sonar Data, 2004), and displayed in echograms. A threshold of –55dB was applied to the data, as we considered unlikely that cells with lower mean volume backscatter strength (Sv) values contained walleye pollock returns (Burgos and Horne, in preparation). Returns from 0.5 m above the sounder detected bottom and 10m below the surface were eliminated from the analysis. Regions of the echogram containing returns from species other than walleye pollock were masked out using virtual echograms (Higginbottom et al., 2000). The acoustic data were echo integrated at a horizontal resolution of 20 m (equivalent to 1-4 pings) and a vertical resolution of 1 m (the minimum vertical resolution available in Echoview). The echo integrated data from each transect were stored as a matrix, where each cell contained the mean volume backscatter strength (Sv) of the volume represented by each 20 m x 1 m area cell. Because each cell in the matrix contained the integrated Sv value of 5-20 of cells from the original echogram, it was possible to have cells in the matrix with Sv values below the –55 dB threshold. Matrix cells corresponding to cells in the original echogram whose values were all below –55 dB were given a value of –999 dB and considered empty “background” cells. Cells below the bottom were given a different value to allow posterior identification. Cells with mean Sv values higher than -39.67 dB (corresponding to a volume backscatter strength of a 40 cm FL walleye pollock and an average separation of one body length) were considered errors in bottom detection or noise in the water column. These cells were coded as empty cells (-999 dB) or as cells below bottom, depending on their position.

2. Selection of length for echogram segmentation.

A critical step in the analysis of spatial pattern is the selection of the appropriate analytic resolution (Gustafson, 1998). Pattern is scale-dependent. The scale of the pattern should match the observation scale (Wiens, 1989). Two factors that influence measures of heterogeneity are resolution of the data, and range of the study area (Horne and Schneider, 1994). We examine spatial patterns at two spatial scales. When computing metrics to quantify spatial heterogeneity in echogram segments, the range is set to the size of a segment and the resolution is a 20 m x1 m bin. After each echogram segment has been characterized and classified, we analyzed the distribution of echogram types over the study area. In this step, the range of our analysis is the area covered by each survey, and the resolution of the data corresponds to the size of an echogram segment. The size of echogram segments should be approximately half of the spatial extent of the patterns being described, as the smallest scale that can be resolved in a spatial or temporal series is twice the resolution of the observations (Legendre and Legendre, 1999).

To select the length of echogram segments, we estimated the extent of small-scale patterns in walleye pollock. The distribution of walleye pollock is potentially influenced by environmental factors (e.g. bathymetry, presence of fronts or upwelling areas) operating at large-scale (10-1000 km) and smaller scale behavioral responses (e.g. vertical migrations or formation of aggregations). To remove the influence of large-scale factors and identify small-scale patchiness, we utilized Generalized Additive Models (GAMs). The distribution of area backscattering strength (Sa) observed in each survey at a horizontal resolution of 20 m was modeled as a function of bottom depth and location:

$$Sa=s(\text{bottom depth})+s(UTMx, UTMy)$$

where s(bottom depth) is a one-dimensional smooth curve representing the relationship with bottom depth, and s(UTMx, UTMy) is a two dimensional smooth surface representing location (expressed in UTM coordinates) and acting as proxy for other location-specific environmental factors. The model was fitted using Generalized Additive Models with penalized regression splines (Wood and Agustin 2002). This method provides flexibility in the selection of the smooth independent functions, and allows for multi-dimensional smooth terms and model selection. In the next step we extracted the residuals of the model and calculated one-dimensional variogram using Cressie's (1993) robust approach. The range of these variograms was considered to represent the extent of small-scale patchiness. Echograms were divided in segments of length approximately half the range of these variograms.

3. Data processing

Echograms from each transect in summer and winter surveys were divided into sections, starting at the beginning of each transect and continuing until the end of the transect. Most transects were intermittently interrupted for fishing or other vessel maneuvers, making these transects continuous in space but not in time. All transect interruptions were identified using data from cruise logs. Whenever an interruption occurred, the current segment was ended and a new segment started after the location of the interruption (Fig. 4). This avoided possible artifacts from echogram segments containing data that was not continuous in time.

Data from each echogram segment were recorded in a binary matrix, a categorical matrix and a raw data matrix. The binary matrix indicated the presence or absence of acoustic density higher than background levels (-999 dB) in each cell and was used to identify patches and to characterize aspects of the spatial heterogeneity of non-empty cells. The categorical matrix contained Sv values classified into eight classes. Class intervals were calculated as

$$CI = meanSv \pm n \cdot \sigma Sv \quad \text{(n=1,2,3…)}$$

where meanSv and σSv are the mean and standard deviation of the mean volume backscatter strength of all cells in each survey. In this way, categories represent degrees of departure from the mean volume backscatter strength in each survey. The categorical matrix was used to characterize aspects of the spatial heterogeneity related to acoustic density. The raw data matrix held the original Sv values from the current echogram segment.

To calculate landscape metric values we utilized Fragstats v 3.0 (McGarigal and Marks, 1995), an application that calculates a large array of landscape metrics from raster maps. Fragstat assumes that cells of the raster map are square. Because the cells in our matrices were rectangular, we changed the resolution of our data to 1x1m by repeating 20 times every column of the binary, categorical, and raw data matrices. In all cases, we coded background cells and cells bellow the bottom (i.e. outside of the landscape boundary) to be recognized as such by Fragstats, as background cells and cells outside the landscape have an effect on the calculation of landscape metrics (McGarigal and Marks, 1995). Additional metrics were calculated using custom written software.

4. Calculation of metrics

A series of metrics were used to quantify spatial distributions of acoustic density: occupancy (i.e. the degree of coverage of acoustic returns on the echogram), fragmentation (i.e. how the acoustic density present in each segment is divided), vertical distribution, and density structure (i.e. how acoustic density values are located, regardless of patch structure). A complete list of the metrics calculated is shown in Table 1.

Several metrics used to characterize spatial heterogeneity in each segment were patch-based and were calculated separately for each patch. In this study, any non-zero cell or any groups of adjacent non-zero cells were considered patches. Adjacency was evaluated using the eight-neighbor rule in which adjacency also includes the diagonal cells. The concept of "patch" is analogous to "schools" or "aggregations" in echo-trace classification, although it is less restrictive because no minimum size criteria were applied. Patches were considered only within the boundaries of each segment. In cases where spatial structures (e.g. large shoals or benthic 'carpets') extended beyond the limits of a segment, only the fraction within the segment was included. Median and median absolute deviations (a robust measure of dispersion) of each patch-based metric were calculated in each segment. Most patch-based metrics were calculated directly using the binary matrix, including patch area, length, height, and distance to nearest neighbor. Some patch-based metrics, such as mean backscatter strength, were calculated using the binary matrix to identify patches and then the raw data matrix was used to obtain Sv values of pixels within each patch.

We also calculated a set of landscape-based metrics, without reference to individual patches. The clumpiness index was calculated using the binary matrix. In addition, we computed the following indices using the categorical matrices: CONTAG, PLADJ and SvR. Values in the categorical matrices represented departure of each cell from the overall Sv mean within the survey. Because these metrics were calculated at the scale of a landscape, they quantify the probability among cells of the same category to be spatially aggregated and the degree of mixing with cells of different categories.

To ensure that all metrics were comparable, all data were normalized using the Box-Cox method (Sokal and Rohlf 1981) and standardized by subtracting the mean normalized value and dividing by its standard deviation previous to all statistical analyses.

5. Redundancy and ordination

It is well known that many indices used to measure spatial heterogeneity are redundant, measuring similar aspects of the spatial pattern (Gustafson, 1998). To measure redundancy among metrics we calculated correlation coefficients among all possible pairs of metrics. To simplify our analysis, when two metrics had a correlation index higher than 0.9, one of the metrics was removed. When multiple metrics had correlation indices higher than 0.9 we removed the metrics with the highest number of pairwise correlations. We then utilized Principal Component Analysis (PCA) to explore relationships among the remaining metrics, and to express metric variability in a reduced number of axes. Only principal components whose eigenvalues were larger than the mean of all eigenvalues were considered significant (Legendre and Legendre, 1999).

6. Typology of spatial patterns

We used cluster analysis to identify groups of transect segments with similar characteristics and to develop a typology of walleye pollock spatial distributions. To divide echogram segments into similar groups we used the partition around medoids (pam) method proposed by Kaufman and Rousseeuw (1990). A number of representative segments, known as medoids, are selected by minimizing the total dissimilarity of all segments to their nearest medoid (Struyf et al., 1997). Segments are assigned to the cluster corresponding to the nearest medoid. We used the pam function in the software package R (R Development Core Team, 2004), which also calculates the average silhouette width, a measure of clustering quality. The optimal number of clusters was selected by conducting cluster analysis with a range of cluster numbers and then selecting the cluster number with the highest average silhouette width (Struyf et al., 1997). Each cluster is considered a distinct type of spatial pattern.

7. Differences in metric values among echogram types

Because the clustering analysis was based on the metrics calculated in each segment, it is not appropriate to use standard analysis of variance to explore differences among metric values in echogram types. Instead, we computed Tukey Honest Significant Differences (HSD, Yandell, 1997) to obtain confidence intervals for each metric on the differences between the means of the metrics among pairs of echogram types. Intervals that included a zero value indicated that the metric did not differ between the pair of echogram types. The number of non-significant pairwise comparisons in each metric was used as a measure of sensitivity of the metric to the patterns classified in each echogram type. To examine the relationship between spatial patterns and environmental variables, we also utilized Tukey HSD to test for differences on the mean bottom depth, and on the mean line backscatter coefficient (Sa) among segments assigned types.

8. Spatial correlation of typologies

Cluster analysis was performed with no reference to spatial locations of each echogram segment. To test if echogram segments of the same type were spatially autocorrelated (this is, if echogram segment types tended to spatially co-occur), we performed a modified Ripley's K test (Ripley, 1981). The distance among all pairs of echogram segments was calculated and classified as distance lags. For each distance lag and each echogram segment type, we calculated the number of pairs of echogram segments belonging to the same type as a fraction of all the echogram segment pairs located within that distance lag. This ratio was used as a similarity index. To test if the number of similar pairs located in each lag distance was higher than what was expected in a random spatial distribution we performed a permutation test. Echogram segment types were randomized among locations, and then the similarity index was re-calculated. This procedure was performed 100 times. If the number of similar pairs observed in each distance lag was higher than the number computed on 95% of the permutations, it was considered to be evidence of spatial aggregation of that type at that distance lag. Analysis was performed separately on the summer and winter survey data.

Results

Optimal length of echogram segments

Generalized Additive Models (GAMs) were used to model the distribution of acoustic density as a function of a smooth function with depth, and a smooth two-dimensional surface with location. For both the summer and winter survey the bottom and location effects were significant (Fig 5, $P < 0.05$). Empirical variograms calculated from the residuals of the GAMs indicated that the scale of aggregation in the summer survey was approximately 2-3 nm (Fig. 6), while in the winter survey the aggregation scale was 4 nm. These results indicate that descriptive metrics calculated in echogram segments 1nm long should adequately describe walleye pollock spatial distribution.

Data processing

A total of 4247 echogram segments were examined after dividing transects from both surveys and removing segments that did not contained walleye pollock acoustic returns. A small number of segments (n=121) were also removed because some of the metrics could not be calculated. As an example, distance to nearest neighbor (NND) could not be computed for segments containing only one patch. The final number of segments included in the analysis was 4126, from which 3751 were from the summer survey and 375 were from the winter survey.

Redundancy

From the original 38 metrics, 9 metrics were removed because they were highly correlated to other metrics. A group of nine metrics (CA, PLAND, ED, LPI, med ENN, NP, PD, SPLIT and LSI - see table 1 for metric names) were highly correlated with two or more metrics within same group. First, NP and CA were removed, leaving PD and PLAND, their versions standardized to the segment area. Next, SPLIT, LSI and ED were also removed because they were correlated to several variables from the group. After removing these metrics, med ENN did not showed high correlation to any of the remaining metrics and was left in the analysis. LPI, PLAND and PD were not removed even they were highly correlated because we considered that they measured important aspects of the spatial patterns in echograms. Med PERIM and mad PERIM were also removed from the analysis because they were highly correlated to med AREA and mad AREA. We also removed med PDEPTH and mad PDEPTH because med PDEPTH was highly correlated to med DEPTH.

Ordination

Principal component analysis was performed on the remaining 29 metrics. Results of the PCA indicated that the first eight components were significant and explained 83% in the variability of the set of metrics (Table 2). The first component explained 33% of the variability and was dominated by metrics related to occupancy, dominance and patch size (PLAND, LPI, med ENN, mad AREA, and mad HEIGHT). The second component explained 18% of the variability and was dominated by metrics related to vertical distribution (med RDEPTH, med PRDEPTH, mad RDDEPTH, mad DEPTH and mad PRDEPTH). The rest of the significant components explained a small fraction of the variability.

Clustering analysis

The partition around medoids method was used to divide the 4126 transect segments into groups and to develop a classification typology. Clusters were detected with a varying number of medoids. The highest average silhouette width was obtained with two medoids, and the next highest value with six medoids (Figure 7). In any case the average silhouette width was higher than 0.25, indicating that there is no clear cluster structure (Struyf et al., 1997). Clustering can be used in this case to create a typology or classification system of clustered objects (Legendre and Legendre, 1989). Even though there was strong evidence for two clusters, we decided to classify the transect segments into six groups because a typology with two types would not be useful. Figure 8 shows the location of the echogram segments assigned to each cluster. Clusters can be distinguished, although there is considerable overlap. It should be noted the two main principal components only represent 51% of the variability in the series, and thus clusters will seem less separated than in the multidimensional space of the 29 metrics. The median values for the metrics calculated in each echogram type are shown in Table 3.

Acoustic typology

A representative echogram segments from each type is displayed in figure 9. Echogram types are briefly described below:

Type 1

A total of 600 segments were classified into Type 1. This type includes echogram segments with the lowest patch density. Patches in echograms of this type are small (in terms of area, height and length), and with reduced variability in all size metrics. The low number and small sizes of patches translates into low occupancy (PLAND) and dominance (LPI) values. The median and the variance of the distance to the nearest neighbor is the highest among all echogram types, which is a consequence of the low number and size of patches. Patches had relatively high mean Sv values, but intermediate SL values. Patches in these echograms segments have relatively high indices of shape complexity (med SHAPE, med FRACTAL), suggesting that most patches have irregular geometric shapes. Nevertheless, visual inspection of echogram segments assigned to this cluster indicates that most patches are formed by a low number of pixels and thus their geometric shape is relatively regular. Variability of complexity indices was small (mad SHAPE and mad FRAC).

Patches in echogram segments were located near the bottom. This type had the highest median path depth (med DEPTH), median relative patch depth (med RDEPTH) and median Sv relative depth (med PRDEPTH). The variability measurements of these three metrics (mad DEPTH, mad RDEPTH and mad PRDEPTH) were the lowest among all types.

The clumpiness index (CLUMPY) was the lowest among all types, indicating that the distribution of non-zero pixels was closest to a random distribution. This type also had a moderate value for the contagion index (CONTAG) and the lowest value for the dispersion index (PLADJ). Finally, Sv richness (SvR), a measure of the range of Sv values, was intermediate. A total of 600 segments were classified into type 1.

Type 2

Type 2 contained a total of 1015 segments. This type included echogram segments with high patch density, moderate occupancy, and moderate dominance values. Patches located in this type had intermediate areas but tended to have relatively large median height. Variance of size metrics was also intermediate. Median distance to the nearest neighbor was relatively low, with moderate variance. Patches in this segment had low mean Sv values but moderate SL values. Measurements of shape complexity suggested that patches in this type had low to moderate geometric complexity, and that variability in the shape complexity of patches was low.

All measures of vertical distribution had intermediate values. Visual inspection of echograms in this type indicated that most patches were located in the lower two third of the water column.

Values for the clumpiness index calculated for echograms of this type were moderate, and tended to be higher than in types 1 and 3. This result indicated a higher tendency for non-zero pixels to be clustered. In most cases, the contagion index was relatively low, while the dispersion index was of intermediate value. Sv richness was the lowest among all section types.

Type 3

Type 3 included 380 segments. Patch-based metrics in this type were similar to those in type 1. Compared to patches in segments of type 1, patches in type 3 were of similar size (area, length and height), but variability in patch area was higher. Although still relatively low, patch density was higher than in segments of type 1, which translates to higher occupancy and dominance indices. Patches in this type had moderate Sv values, but low SL values. Median distance to nearest neighbor was lower than in type 1, although variability was similar. Values of median and variance in shape complexity indices were similar than those in type 1 section. In type 3 sections, visual inspection also indicated that patches were small and formed by few pixels, and that values of shape complexity indices were misleading.

Metrics related to vertical distribution differed between echogram segments of type 1 and type 3. Although median patch depth was similar between these two types, variability in patch depth in type 3 was the highest among all types. The median patch relative depth and the median pixel relative depth were, together with segments 5 and 6, the highest among all echogram types. This indicates that patches in segments of this type are more widely spread through the water column.

The clumpiness index in type 3 sections was higher than in type 1 sections, suggesting that a higher degree of clustering of non-zero cells occurred. Also compared with type 1, the contagion index was lower, while the dispersion index was higher. Sv richness was lower than in type 1, indicating that there is less variability in Sv values in the cells of type 3 echograms.

Type 4

A total of 350 segments were classified into type 4. Echogram segments assigned to this type had moderate patch density, but had high occupancy and dominance indices. Patches in this echogram type were large, as evidence by the highest med AREA, med LENGTH, and med HEIGHT among all types. Values for mean Sv and SL were the highest among all types. Distances among patches were relatively small, as evidenced by low NND values. Variability in NND was intermediate. Shape complexity indices indicated that patches were geometrically complex, and that variability in shape complexity was high.

Vertical distribution metrics indicated that patches in segments of this type were located in a narrow band near the bottom. Values of med RDEPTH and med PDEPTH were only lower in type 1, whereas values of med DEPTH were (together with types 1 and 3), the lowest among all types. All measures of variability in depth distribution were low.

This type had the highest clumpiness index values, indicating high levels of aggregation. The contagion index was the lowest among all types, while the dispersion index and Sv richness were relatively high.

Type 5

Type 5 included a total of 341 segments. This type contained echograms with intermediate patch density, but relatively low occupancy and dominance indices. Patches were intermediate in size and had similar characteristics to patches in type 2. Mean Sv and SL values were intermediate. Distances to nearest neighbor were large and highly variable. Shape complexity indices were very low, indicating that patches have relatively simple geometric shapes. Variability in patch complexity was also low.

A notable characteristic of this echogram segment type is that all vertical distribution metrics indicate that patches are distributed throughout the water column. Together with type 6, median patch depth was the highest among all types. In addition, med RDEPTH and med PDEPTH were (together with types 3 and 6) the highest among all types. Variability indices indicated a moderate to high variability in the vertical distributions of patches in this type.

The moderate value of the clumpiness index indicates that non-zero pixels are more aggregated in this echogram type than in types 1,2, and 3; but less aggregated than in types 4 and 6. Values of the contagion index were moderate, while the dispersion index was relatively high. Sv richness was relatively low.

Type 6

A total of 1440 segments were classified into type 6, making it the largest category. Echogram segments of this type had the highest patch density, and the largest occupancy and dominance indices. Patch size was smaller than in segments of type 4, but larger than in any other type. Mean Sv and SL values were intermediate and very similar to type 5. This type also had the lowest distance to the nearest neighbor. Variability in NND was also very small. Shape indices indicate that patches in echograms of type 6 had, on average, moderate but highly variable shape complexity. Most of the patches in segments of this type were located near the bottom, although variability in vertical distribution was high.

Non-zero pixels in segments of type 6 were highly aggregated. Values for the contagion index were moderate. Dispersion and Sv richness was the highest among all types.

Visual inspection of a random sample of echogram segments of the six types shows that patterns assigned to each type are consistent. Type 1 included segments with low acoustic density and with small patches located near the bottom. Segments of type 2 had patches of moderate size but low density, located in the lower two thirds of the water column. Type 3 included very diffuse epibenthic layers, with small patches occupying the bottom half of the water column. Echogram segments of type 4 had well defined schools, or relatively compact benthic and epipelagic layers. Type 5 included segments with diffuse layers occupying most of the water column. Finally, segments of type 6 had dense layers occupying the bottom half of the water column. Nevertheless, visual inspection of echogram segments assigned to each group revealed that with some frequency segments were classified into types that did not match their general characteristics. In addition, the cluster analysis grouped spatial patterns that seem to be fairly distinct. For example, segments with benthic carpets and with isolated, well-defined schools were included together in type 4.

Sensitivity

The number of non-significant pairwise comparisons of each metric among echogram types was used as a measure of metric sensitivity (Table 4). Measurements of central tendency and variability of patch-based metrics were less sensitive to echogram types than landscape metrics calculated without reference to patches. The metrics with lowest sensitivity were mad LENGTH (10 non-significant comparisons from a total of 15), mad PMEAN (7 non-significant comparisons) and med LENGTH (6 non-significant comparisons).

Relationship to bottom depth and total acoustic density

Results from Tukey HSD indicated that echogram segments of type 6 and 4 are related to locations with the highest Sa values. Segments of types 1 and 3 tended to have the lowest Sa values. These results are consistent with metric values observed in these echogram types. Types 6 and 4 had high patch density and coverage indices, indicating that acoustic density was high. Types 1 and 3 had low patch density and coverage indices, indicating that acoustic density was low. Echogram segments of type 3 were associated with relatively deeper bottom depths, while segments of type 2 and 6 were more common in shallower waters.

Spatial analysis

Results of the modified Ripley's K test indicated that echogram segment types were spatially autocorrelated. The degree of spatial autocorrelation varied among segment types. In the summer survey, segments of types 1 and 3 were autocorrelated at scales below 50 km (Fig 10). Autocorrelation distances for segments of type 4 and 5 were in the order of 40km. Segments of type 6 were autocorrelated at scales up to 150 kilometers. In contrast, echogram segments of type 2 had a short autocorrelation distance (~10km). In the winter survey echograms of type 6 had the largest autocorrelation distance (40 km, Fig 11). Autocorrelation distances for types 2 and 4 were approximately 10-15 km. Echogram segments of type 1, 3 and 5 showed little autocorrelation.

Spatial locations of echogram segments differed among types. During the summer survey, segments of type 1and 4 were more common in areas north of the Aleutian Islands, in the southeast of the sampling area, and on the northwest end of the area surveyed (Fig 12). Segments of types 3 and 5 were more frequent in the southwest of the sampling area, with type 5 segments were more widely distributed. Segments of type 6 were more common in the center and the northwest of the surveyed area. Segments of type 2 were distributed across the sampling area. Although the area covered by the winter survey was smaller that the summer survey, differences in the spatial location of echogram segment types were apparent (Fig 13). Segments of type 1 were more frequent in the north. Segments of type 3 were more common in the south of the area surveyed, with type 6 more frequent in the center of the survey area. Types 2, 4 and 5 were distributed across the sampling area.

Discussion

Landscape metrics were used to quantify spatial pattern of fish density data in echograms. Several authors have suggested that landscape metrics capture some aspects of spatial pattern, and that ordination techniques are necessary to identify these aspects (Li and Reynolds, 1994; Riiters et al., 1995; McGarigal and McComb, 1995). Our results support this idea. Principal component analysis indicated that approximately half of the variance in the metrics was explained by the first two components. The first principal component was dominated by metrics describing patch density, occupancy and dominance. Metrics related to the vertical distribution of patches were prevalent on the second principal component. Other aspects of spatial patterns in echograms, like the distribution of acoustic density, represented a smaller fraction of the total variance. These results suggest that echogram segments in this study can be located along two main gradients: one representing the degree of occupancy of acoustic density and other representing the vertical distribution.

The classification typology developed for walleye pollock in this study was consistent. Nevertheless, the cluster structure of metrics was relatively weak, as shown by the low average silhouette width value, and the visible overlap among clusters when members were plotted along the first two principal component axes. It was not surprising that visual examination of segments assigned to each echogram type revealed overlap among spatial patterns assigned to each type. As an example, sections with low density pelagic and benthic layers were assigned to types 2 and 3. In addition, high-density pelagic layers were more frequent in type 4, but were also classified as type 6. Another consequence of the weak cluster structure is that distinct spatial patterns were included in the same type. Well-defined schools, dense midwater layers, and benthic 'carpets' were included in type 4. Additional work is necessary to optimize the set of metrics necessary to minimize the overlap among categories.

An important aspect to consider when selecting metrics that quantify spatial pattern is the sensitivity of metrics when detecting differences in distribution patterns. Metrics that do not vary when distributions vary are of limited use. Several authors have quantified the sensitivity of metrics used in landscape analysis (e.g. Neel et al., 2004). The sensitivity of our metrics was evaluated by tabulating the number of non-significant pairwise comparisons of each metric among spatial pattern types. Metrics with low sensibility to spatial pattern categories would tend to be similar among types. The resulting number of non-significant pairwise comparisons will be higher. Results indicate that patch-based metrics (i.e. median and median absolute deviation of metrics calculated in individual patches) had less sensitivity than landscape-based metrics. We attributed this to the fact that echogram sections were located within a continuum of patch density, coverage, and dominance index values. As an example, sections of type 1 and 3 tended to have few small patches, resulting in low coverage and dominance. When acoustic density in sections increased (as in sections of type 4 and 6), patch density and occupancy values also increased. Dominance index values also increased, suggesting that the size distribution of patches became more skewed. Yet, median patch area did not vary among echogram types, indicating that even in sections with high acoustic density there were considerable numbers of small patches. As a result, median values of patch-based metrics were strongly influenced by the characteristics of small patches, making these metrics less sensitive to the presence of large patches. The same applies to the median average deviation of patch-based metrics, as they were calculated using the median as measure of central tendency. To increase the sensitivity of patch-based metrics, measurements of central tendency should reflect properties of larger patches. One possibility is to use area-weighted means. The use of metrics with higher sensitivity will translate to a better-defined cluster structure and a more consistent classification typology.

Measures of shape complexity were difficult to interpret and could have contradictory values. In echogram sections with small patches, shape complexity indices suggested that patches had complex geometrical shapes. In theory, the SHAPE index approaches a value of 1 for regular forms, increasing when the perimeter of the patch becomes more irregular (McGarigal and Marks, 1995). In the same way, the fractal dimension index should range between 1 when patch shape is very regular and approach 2 when the shape is highly complex. When patches were very small, values of both indices increased regardless of patch shape. For example, the smallest patch possible in our data is a single pixel: a rectangular patch of 20m x 1 m. For this patch, the value of SHAPE is 2.35 and the value of FRAC is 1.57. These numbers suggest a moderately complex geometrical shape. High median SHAPE and FRAC values indicate high shape complexity of patches within a segment, or may be an artificial value due to the presence of a large number of small patches.

Values obtained for the contagion index (CONTAG) and the percentage of likely adjacencies (PLADJ) were also difficult to interpret. Both indices are measures of aggregation. Yet, echogram sections with high CONTAG values had low PLADJ values. The CONTAG index measures both contagion (e.g. the tendency of cells of the same category to be aggregated) and interspersion (e.g. how much groups of pixels in the same category are mixed with groups of cells in other categories, Li and Reynolds, 1993). The highest contagion values were obtained in echograms types 3, 5 and 6, which included sections with low and very high patch density. It is apparent that the tendency of cells within Sv categories occurring together is independent of patch size. The PLADJ index measures the degree of aggregation of groups of pixels in the same category. Contrary to CONTAG, it is not affected by interspersion, but can be influenced by patch shape (McGarigal and Marks, 1995). In our data PLADJ is also related to patch size. Additional work is necessary to fully understand the relationship between CONTAG and PLADJ indices.

Results from the spatial analysis indicate that echogram types are spatially autocorrelated and that the scale of autocorrelation and the geographical location varies among types. This suggests that there may be environmental factors influencing spatial patterns detected in each of the echogram types. Swartzman et al. (1994) reported that walleye pollock aggregation patterns are influenced by bottom depth, depth of the thermocline, and location of fronts. Our results suggest that echogram types were related to bottom depth, but the influence of other environmental variables has not been explored.

This paper represents our first attempt to quantify spatial heterogeneity of acoustic data in echograms using landscape and other metrics. Further work includes the optimization of metrics so they fully capture differences in spatial pattern allowing increasing the accuracy of the classification typology. It is also necessary to quantify the sensibility of these methods to changes in echogram segment size and on the transect starting point, two factors known to influence the results of moving windows analysis on spatial or temporal series (Horne and Schneider, 1995). Our results suggest that the methods developed in this paper could be used to quantify and classify spatial heterogeneity of acoustic data from any species, regardless of its spatial patterns. For species that form well-defined aggregations, this methodology can complement results from echo-trace classification by quantifying the spatial distribution around detected aggregations. In the case of echograms where acoustic returns from multiple species are separated in space, the analysis can be carried out for each species and for the echogram as a whole. Spatial relations among patches of different species can be quantified. In all cases the study of correlation among metrics describing spatial pattern and environmental variables is a promising approach that could provide information on factors that influence small-scale distribution of aquatic organisms.

References

Bertrand, A., F.X. Bard, and E. Josse. 2002. Tuna food habits related to the micronekton distribution in French Polynesia. Marine Biology 140: 1023-1037

Burgos, J.M. and J.K. Horne. In prep. Sensitivity analysis of an aggregation recognition algorithm for acoustic data.

Cressie, N.A.C. 1993. Statistics for Spatial Data, Wiley-Interscience, New York. 928 pp.

Gauthier, S. and G.A. Rose. 2002. Acoustic observation of diel vertical migration and shoaling behaviour in Atlantic redfishes. Journal of Fish Biology 61: 1135-1153.

Gustafson, E. J. 1998. Quantifying landscape spatial pattern: what is the state of the art? Ecosystems 1: 143-156

Higginbottom, I.R., T.J. Pauly and D.C. Heatley. 2000. Virtual echograms for visualization and post-processing of multiple-frequency echosounder data. Proceedings of the Fifth European Conference on Underwater Acoustics (Ed. M.E. Zakharia): 1497-1502.

Honkalehto, T. and S. de Blois. 2001. Walleye pollock (*Theragra chalcogramma*) abundance on the southeastern Bering Sea shelf and in the Aleutian Basin near Bogoslof Island in February and March, 2000. NOAA Technical Memorandum NFMS-AFSC-125,-126

Horne, J.K. and D.C. Schneider. 1994. Analysis of scale-dependent processes with dimensionless ratios. Oikos 70: 201-211

Horne, J.K. and D.C. Schneider. 1995. Spatial variance in ecology. Oikos 74: 18-26

ICES. 2000. Report on Echo Trace Classification. ICES Cooperative Research Report No. 238. 107 pp.

Kaufman, L. and P.J. Rousseeuw. 1990. Finding groups in data: an introduction to cluster analysis. Wiley-Interscience. New York. 368 pp.

Legendre, P. and L. Legendre. 1999. Numerical ecology, 2nd edition. Elsevier Science, New York. 870 pp.

Li, H. and J.F. Reynolds. 1993. A new contagion index to quantify spatial patterns of landscapes. Landscape Ecology 8: 155-162

Li, H. and J.F. Reynolds. 1994. A simulation experiment to quantify spatial heterogeneity in categorical maps. Ecology 75: 2446-2455

McGarigal, K, and B.J. Marks. 1995. FRAGSTATS: spatial pattern analysis program for quantifying landscape structure. Gen. Tech. Report PNW-GTR-351, USDA Forest Service, Pacific Northwest Research Station, Portland, OR

Misund, O.A. 1997. Underwater acoustics in marine fisheries and fisheries research. Reviews in Fish Biology and Fisheries 7: 1-34

Neel, M. C., K. McGarigal, and S.A. Cushman. 2004. Behavior of class-level landscape metrics across gradients of class aggregation and area. Landscape Ecology 19: 435-455

R Development Core Team. 2004. R: A language and environment for statistical computing. R Foundation for Statistical Computing, Vienna, Austria. ISBN 3-900051-07-0, URL http://www.R-project.org.

Reid, D., C. Scalabrin, P. Petitgas, J. Masse, R. Aukland, P. Carrera, and S. Georgakarakos, 2000. Standard protocols for the analysis of school based data from echo sounder surveys. Fisheries Research 47: 125-136

Riitters, K. H., O'Neill, R. V., Hunsaker, C. T., Wickham, J. D., Yankee, D. H., Timmins, S. P., Jones, K. B., and Jackson, B. L. 1995. A factor analysis of landscape pattern and structure metrics. Landscape Ecology 10: 23-39

Ripley, B.D. 1981. Spatial statistics. Wiley, New York. 272 pp.

Rose, G.A., B. deYoung, and E.B. Colbourne. 1995. Cod (*Gadus morhua*) migration speeds and transport relative to currents on the north-east Newfoundland Shelf. ICES Journal of Marine Sciences 52: 903-913

Schumaker, N. H. 1996. Using landscape indices to predict habitat connectivity. Ecology 77: 1210-1225

Sokal, R.R. and F.J. Rohlf. 1981. Biometry. Freeman and Company, New York. 859 pp.

SonarData. 2004. Echoview. Version 3.10.129. <http://www.sonardata.com/sonardata/WebHelp/Echoview.htm>. Tasmania, Austraila. Accessed July 12, 2004

Struyf, A., M. Hubert and P.J. Rousseeuw. 1997. Integrating robust clustering techniques in S-plus. Computational Statistics & Data Analysis 26: 17-37

Swartzman, G., W. Stuetzle, K. Kulman and M. Powojowski. 1994. Relating the distribution of pollock schools in the Bering Sea to environmental factors. ICES Journal of Marine Sciences 51: 481-492

Teixidó, N., J. Garrabou and W.E. Arntz. 2002. Spatial pattern quantification of Antartic benthic communities using landscape indices. Marine Ecology Progress Series 242: 1-14

Vabø, R. and L. Nøttestad, 1997. An individual based model of fish school reactions: predicting antipredator behaviour as observed in nature. Fisheries Oceanography 6: 155-171

Wiens, J.A., 1989. Spatial scaling in ecology. Functional Ecology 3: 385-397

Wood, S.N. And N.H. Augustin. 2002. GAMs with integrated model selection using penalized regression splines and applications to environmental modelling. Ecological Modelling 157: 157-177

Yandell, B. S. 1997. Practical Data Analysis for Designed Experiments. Chapman & Hall. 440 pp.

Table 1. Indices used to quantify spatial heterogeneity in echogram sections. Patch-based metrics were calculated for each patch individually. Mean (med) and median absolute deviation (mad) of patch-based metrics were calculated to quantify the distribution of metrics in each echogram section. Landscape based metrics were calculated in each section with no reference to patches. (*) Refer to McGarigal and Marks (1995) for details on index calculation.

Index name (units)	Abbreviation	Description
Patch-based metrics		
Area (m^2)	med/madAREA	Patch area.
Length (m)	med/madLENGTH	Patch length
Height (m)	med/madHEIGHT	Patch height
Perimeter (m)	med/madPERIM	Patch perimeter
Shape index	med/madSHAPE	Ratio between patch perimeter and the perimeter of a square with the same area (*)
Fractal dimension index	med/madFRAC	Twice the ratio of the patch perimeter to the patch area, both in logarithmic scale (*)
Euclidean distance to nearest neighbor (m)	med/madENN	Shortest distance to a neighboring patch (*)
Mean Sv (dB re 1 m^{-1})	med/madSVMEAN	Mean volume backscatter strength of cells within the patch
Line backscatter strength (dB re 1m)	med/madSL	Measure of the total acoustic density contained within each patch.
Patch depth (m)	med/madDEPTH	Depth of patches, measured from the surface to the center of the patch.
Relative patch depth	med/madRDEPTH	Same as above but expressed as a fraction of bottom depth.
Landscape based metrics		
Cover area (m^2)	CA	Sum of patch areas (*)
Percentage of landscape	PLAND	Sum of patch areas, expressed as a percentage of the total landscape area (*)
Number of patches	NP	Number of patches in the landscape (*)
Patch density (m^{-2})	PD	Number of patches per unit area of landscape (*)
Largest patch index	LPI	Area of the largest patch as a fraction of the total landscape area (*)
Edge density (m^{-1})	ED	Total perimeter length of all patches divided by the total landscape area (*)
Clumpiness index	CLUMPY	Measure of clustering or aggregation (*)
Splitting index	SPLIT	Measure of patch fragmentation (*)
Normalized landscape shape index	NLSI	Total edge adjusted for the size of landscape and the total area of patches (*)
Average pixel depth (m)	med/mad PDEPTH	Depth of non-zero pixels
Average pixel relative depth	med/mad PRDEPTH	Same as above but expressed as a fraction of bottom depth.
Contagion index	CONTAG	Measurement of class contagion (*)
Percentage of like adjacencies	PLADJ	Measurement of class dispersion (*)
Sv richness	SvR	Number of Sv categories (*)

Table 2. Results of Principal Component Analysis performed on 29 metrics and 4126 echogram sections. Only eigenvalues and loadings for the eight significant axis are shown. Asterisks indicate correlation among metric and axis. ***>0.7>**>0.6>*>0.5. See table 1 for metric names.

	Comp.1	Comp.2	Comp.3	Comp.4	Comp.5	Comp.6	Comp.7	Comp.8
Standard deviation	3.01	2.18	1.43	1.34	1.23	1.09	1.05	1.03
Proportion of Variance	0.33	0.17	0.08	0.07	0.06	0.04	0.04	0.04
Cumulative Proportion	0.33	0.51	0.58	0.65	0.70	0.75	0.79	0.83
med AREA	-0.22 **	0.24 *	0.17	0.08	-0.1	-0.1	-0.07	0.07
mad AREA	-0.23 ***	0.22	-0.02	0.11	-0.06	-0.12	-0.22	-0.05
med SHAPE	0	0.1	-0.45 **	0.28	0.14	-0.12	-0.24	-0.17
mad SHAPE	-0.23 ***	0.14	-0.12	0.03	-0.14	-0.22	-0.14	-0.1
med FRAC	0.19 *	-0.02	-0.41 *	0.22	0.18	0.01	-0.09	-0.06
mad FRAC	-0.23 **	0.1	0.06	-0.04	-0.18	-0.18	-0.32	-0.13
med ENN	0.27 ***	0.05	0.29	-0.01	0.05	-0.07	-0.18	0.04
mad ENN	0.15	-0.03	0.24	-0.16	0.11	-0.02	-0.48 *	0.15
med Sv_mean	0.07	0.2	0.14	-0.08	0.33	-0.25	0.3	-0.4
mad Sv_mean	0.03	0.08	-0.07	-0.37 *	0.41 *	0.09	-0.2	0.12
med SL	-0.03	0.27 **	0.15	-0.04	0.3	-0.22	0.28	-0.37
mad SL	-0.07	0.16	-0.11	-0.27	0.39 *	0.18	-0.19	0.08
med Length	-0.02	0.3 **	0.09	0.4 *	0.2	0.04	0.08	0.36
mad Length	-0.02	0.3 **	0.06	0.4 *	0.22	0.05	0.09	0.39
med Height	-0.24 ***	0.18	0.21	-0.02	-0.15	-0.1	-0.05	0.03
mad Height	-0.24 ***	0.13	-0.03	0.01	-0.07	-0.05	-0.19	-0.12
med Depth	0.11	0.08	0.06	0.29	0	0.34	-0.3	-0.46
mad Depth	-0.18 *	-0.26 *	0.12	0.17	0.2	0.02	-0.15	-0.15
med Rdepth	0.2 **	0.28 **	-0.14	-0.11	-0.17	0.08	-0.08	-0.03
mad Rdepth	-0.22 **	-0.27 *	0.05	0.06	0.18	-0.12	-0.07	0.03
med PRDepth	0.16 *	0.28 **	-0.2	-0.14	-0.22	0.1	0	-0.01
mad PRDepth	-0.18 *	-0.27 *	0.08	0.08	0.23	-0.17	-0.1	0.06
PLAND	-0.28 ***	-0.02	-0.22	-0.06	0.01	0.07	0.14	0.04
PD	-0.25 ***	-0.12	-0.25	-0.09	-0.01	-0.15	0.1	0.09
LPI	-0.26 ***	0.06	-0.19	-0.09	0	0.22	0.16	0.05
CLUMPY	-0.23 **	0.13	0.22	-0.08	-0.03	0.38	0.07	-0.06
CONTAG	0	-0.25 *	0	0.26	0.01	0.23	0.05	-0.15
PLADJ	-0.22 **	0.01	0.15	0.04	0.02	0.48 *	0.05	-0.12
PR	-0.17 *	0.07	-0.15	-0.19	0.19	0.16	-0.06	-0.02

Table 3. Median values of metrics by echogram segment type. Values between brackets are the 10% and 90% percentiles.

	Type 1	Type 2	Type 3	Type 4	Type 5	Type 6
med AREA	20 [20-40]	40 [40-40]	20 [20-40]	60 [40-100]	40 [40-40]	40 [40-40]
mad AREA	0 [0-15]	30 [30-30]	0 [0-30]	59 [30-100]	15 [0-30]	30 [30-30]
med SHAPE	2.3 [2.3-2.3]	2.3 [2.1-2.3]	2.3 [2.3-2.3]	2.3 [2.3-2.8]	1.7 [1.7-2]	2.3 [2.2-2.3]
mad SHAPE	0 [0-0.48]	0.53 [0.19-0.95]	0 [0-0.22]	0.68 [0.26-1]	0.21 [0-0.53]	0.89 [0.43-0.95]
med FRAC	1.6 [1.6-1.6]	1.5 [1.3-1.6]	1.6 [1.6-1.6]	1.5 [1.3-1.6]	1.3 [1.3-1.4]	1.4 [1.3-1.5]
mad FRAC	0 [0-0.1]	0.14 [0.085-0.21]	0 [0-0.063]	0.12 [0.06-0.19]	0.066 [0-0.16]	0.15 [0.11-0.19]
med ENN	61 [21-320]	15 [4.1-61]	21 [5-110]	21 [3-160]	22 [7-190]	3.2 [2.2-8]
mad ENN	30 [0-130]	10 [1.7-31]	17 [2.6-75]	3.2 [0-45]	15 [1.7-85]	1.7 [0.35-7.4]
med Sv_mean	-56 [-61--50]	-58 [-60--55]	-58 [-61--55]	-56 [-59--51]	-58 [-60--54]	-58 [-60--57]
mad Sv_mean	5.4 [2.1-9.2]	5.1 [3.5-7.3]	4.5 [2.5-7.6]	4.8 [2.8-7.7]	4.8 [2.5-6.8]	4.7 [3.7-6]
med SL	-42 [-47--35]	-42 [-44--38]	-44 [-47--40]	-38 [-42--32]	-42 [-45--38]	-42 [-44--40]
mad SL	6.1 [2.3-10]	7.2 [4.9-10]	6 [3.4-8.8]	8.2 [4.2-13]	5.9 [3-8.5]	7.1 [5.8-8.8]
med Length	20 [20-20]	20 [20-20]	20 [20-20]	40 [30-40]	20 [20-20]	20 [20-20]
mad Length	0 [0-0]	0 [0-0]	0 [0-0]	30 [15-30]	0 [0-0]	0 [0-0]
med Height	1 [1-1.5]	2 [2-2]	1 [1-1]	2 [2-3]	2 [2-2]	2 [2-2]
mad Height	0 [0-0]	1.5 [0-1.5]	0 [0-0]	1.5 [0-2.2]	0 [0-1.5]	1.5 [1.5-1.5]
med Depth	100 [68-290]	95 [67-130]	110 [64-180]	100 [71-160]	86 [56-120]	82 [59-110]
mad Depth	0.74 [0-4.5]	5.4 [0.74-15]	15 [6.3-40]	2.6 [0.49-13]	12 [1.5-26]	14 [7.4-24]
med Rdepth	1 [0.98-1]	0.95 [0.84-0.99]	0.84 [0.57-0.95]	0.98 [0.88-1]	0.82 [0.57-0.99]	0.82 [0.69-0.91]
mad Rdepth	0.0047 [0-0.019]	0.054 [0.008-0.12]	0.1 [0.039-0.23]	0.016 [0.0018-0.11]	0.11 [0.015-0.22]	0.14 [0.081-0.22]
med PRDepth	0.99 [0.97-1]	0.96 [0.84-0.99]	0.83 [0.53-0.94]	0.97 [0.86-0.99]	0.82 [0.57-0.97]	0.84 [0.73-0.94]
mad PRDepth	0.01 [0-0.03]	0.039 [0.014-0.1]	0.092 [0.031-0.23]	0.02 [0.0048-0.071]	0.089 [0.019-0.19]	0.097 [0.047-0.18]
PLAND	0.12 [0.026-0.44]	0.94 [0.24-2.2]	0.32 [0.061-1.5]	1.2 [0.095-4.9]	0.52 [0.06-2.1]	4.3 [2-11]
PD	39 [11-110]	160 [46-340]	85 [20-330]	99 [15-290]	120 [13-420]	500 [230-880]
LPI	0.029 [0.0078-0.072]	0.11 [0.045-0.3]	0.044 [0.015-0.17]	0.23 [0.04-1.4]	0.06 [0.018-0.19]	0.44 [0.12-3.9]
CLUMPY	0.62 [0.54-0.69]	0.71 [0.67-0.79]	0.66 [0.6-0.73]	0.76 [0.67-0.85]	0.73 [0.69-0.81]	0.74 [0.69-0.82]
CONTAG	39 [31-53]	38 [31-46]	48 [39-61]	36 [29-43]	40 [34-51]	41 [36-47]
PLADJ	48 [48-55]	55 [52-59]	55 [49-60]	57 [51-64]	56 [52-63]	57 [54-63]
PR	4 [2-5]	4 [4-5]	4 [3-5]	5 [3.9-5]	4 [3-5]	5 [4-5]

Table 4. Number of pairwise comparisons with no significant differences, from 15 possible comparisons among 6 echogram segment types. High number of no significant differences indicate that the metric has low sensitivity.

Metric	n
mad Length	10
mad Sv Mean	7
med Length	6
med SL	5
med Sv Mean	4
mad SL	4
med Depth	4
med Area	3
mad ENN	3
med Height	3
med Rdepth	3
PD	3
med Shape	2
mad Frac	2
Med PRDepth	2
Mad PRDepth	2
mad Area	1
mad Shape	1
med Frac	1
med ENN	1
mad Height	1
mad RDepth	1
LPI	1
CONTAG	1
PLADJ	1
PR	1
mad Depth	0
PLAND	0
CLUMPY	0

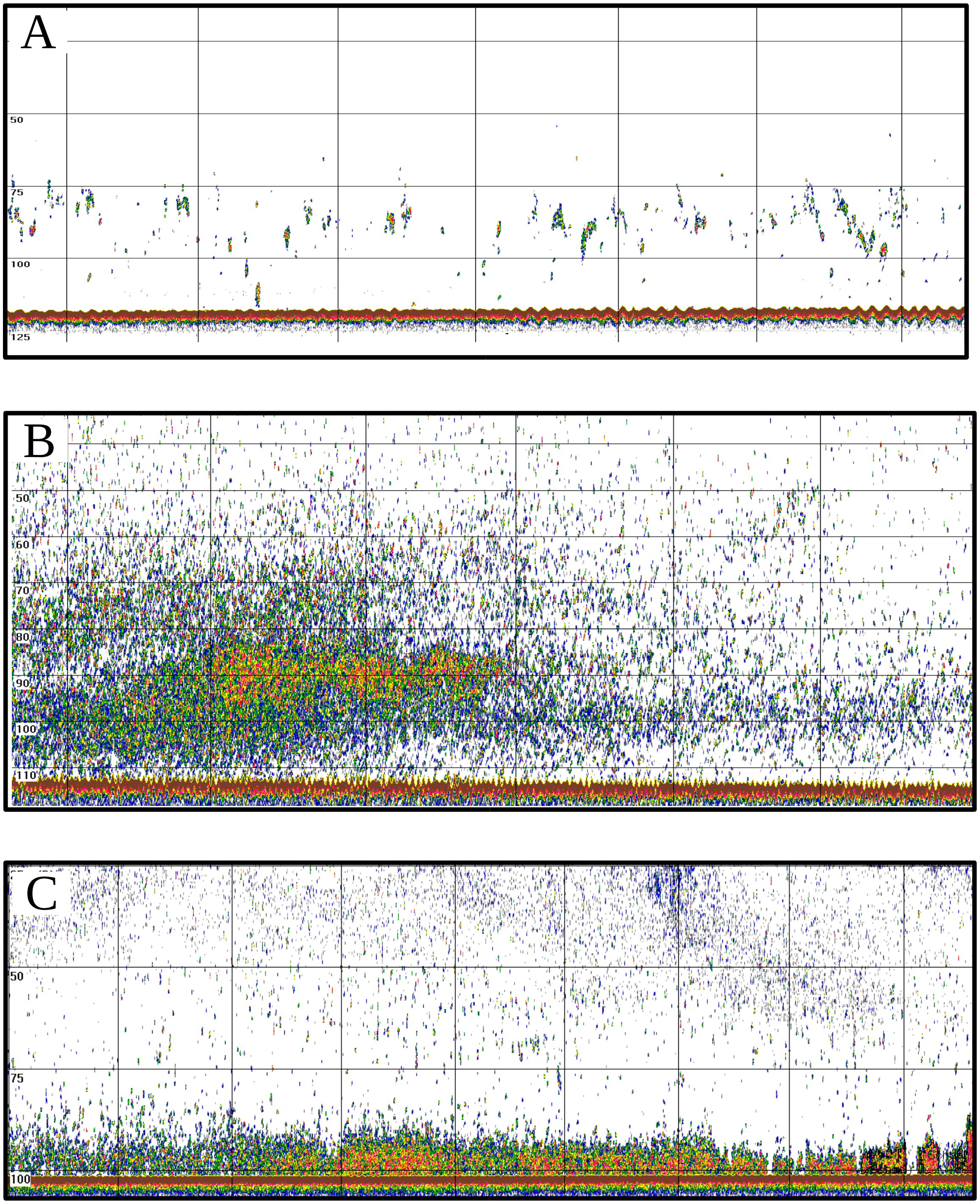

Fig. 1. Examples of walleye pollock spatial patterns: well-defined schools (A), diffuse midwater layer (B), and benthic 'carpet' (C). The grid resolution is 0.5 nm in the horizontal direction and 25 m in the vertical direction.

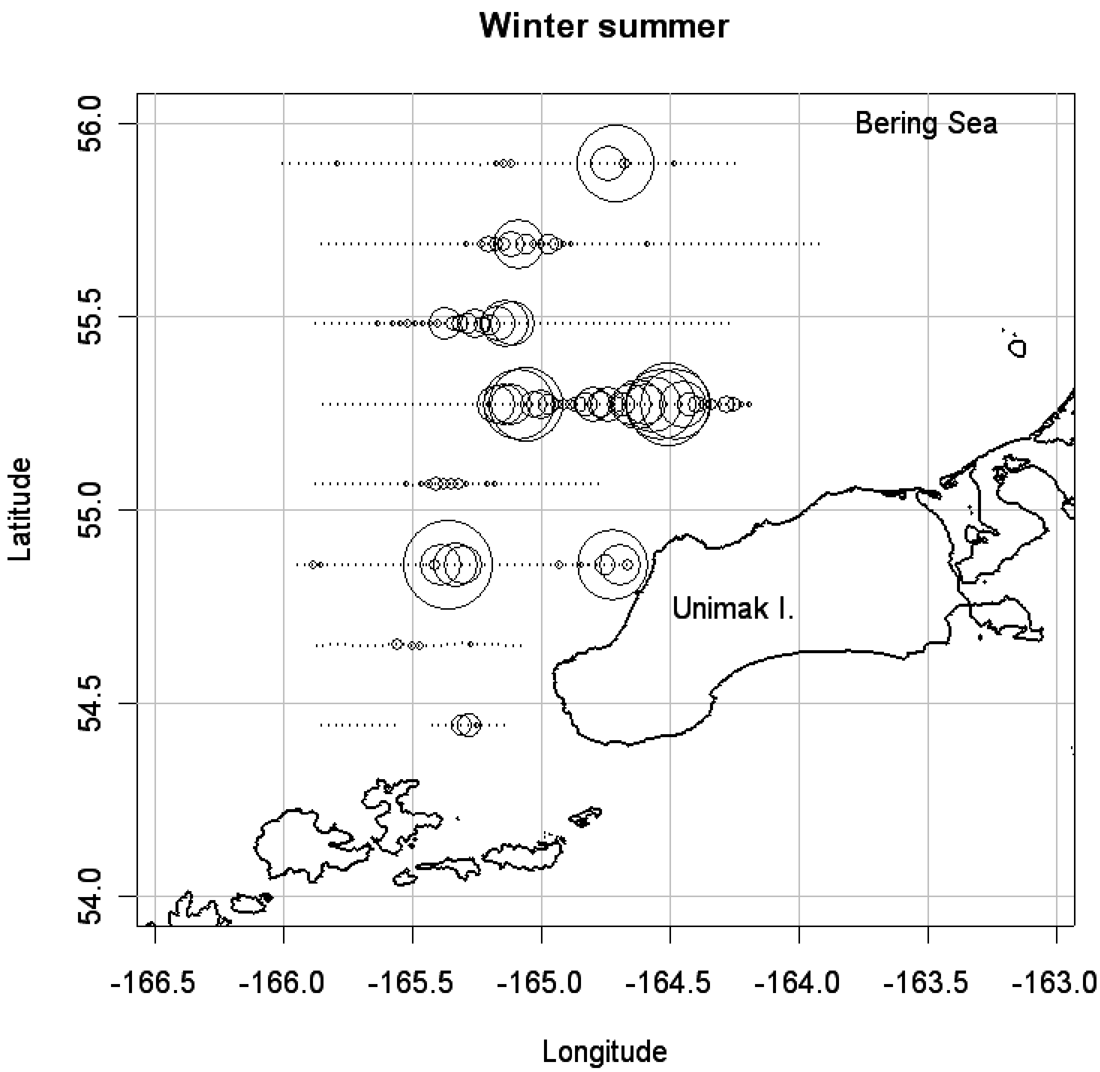

Fig. 2. Track of the winter 2000 survey. Only transects used in this study are included. Radius of circles is proportional to the area backscatter strength from 1nm transect segments.

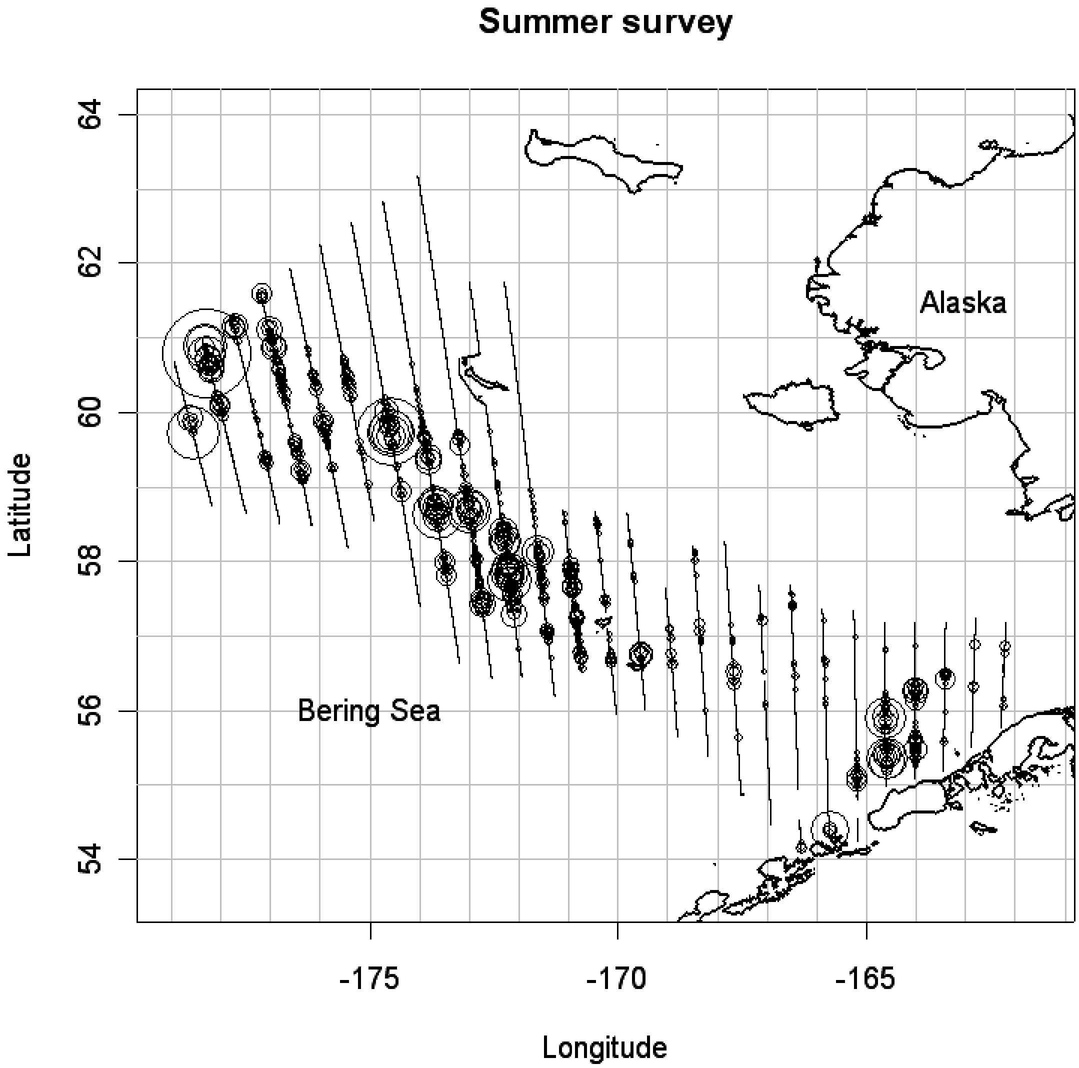

Fig. 3. Track of the summer 2000 survey. Only transects used in this study are included. Radius of circles is proportional to the area backscatter strength from 1nm transect segments.

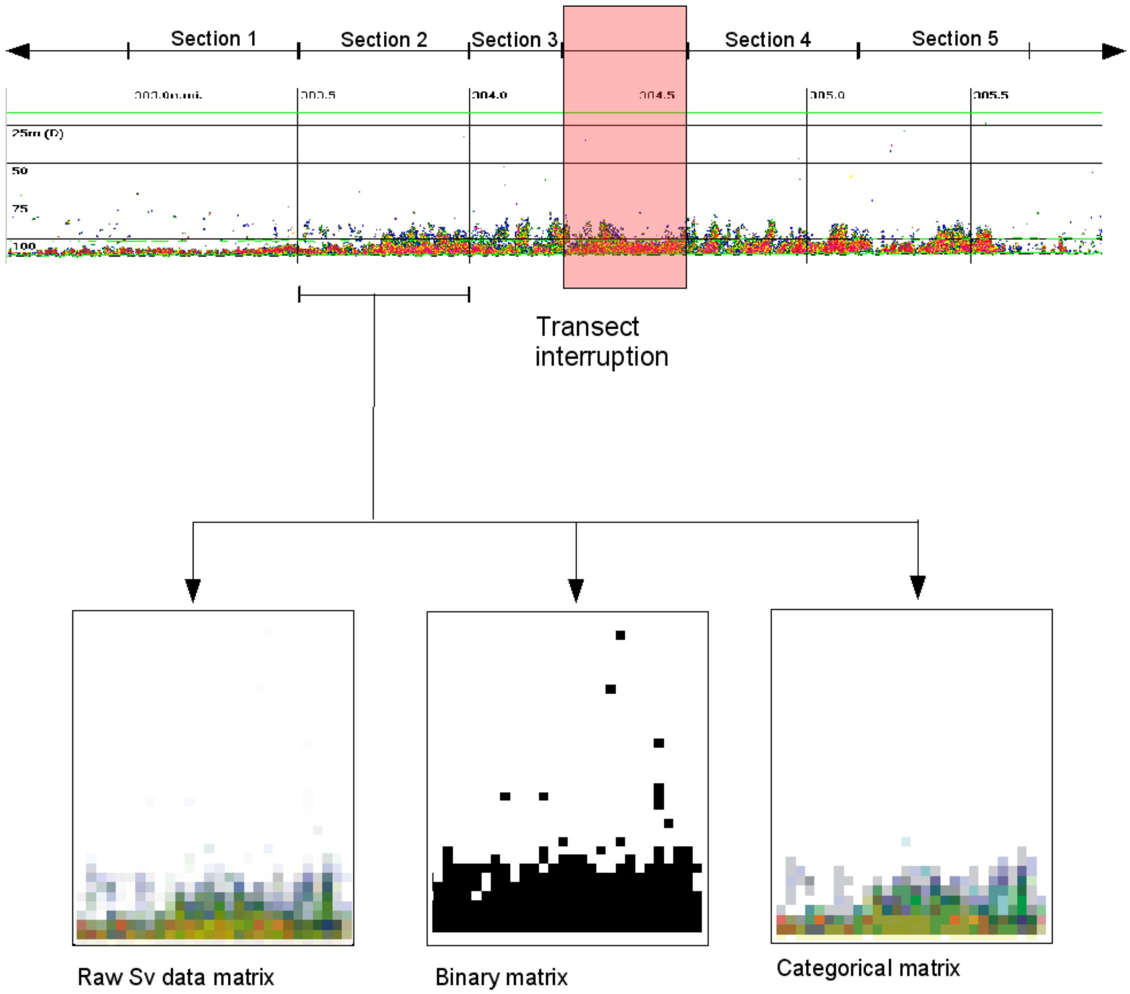

Fig. 4. Scheme of steps in data processing. Transects were divided in sections 1 nm long. On the locations where the transect was interrupted (e.g. due to fishing maneuvers) a new section was initiated. Data in each section was echo-integrated at a resolution 20 m x1 m, and resampled to have resolution of 1 m x 1m. The data from each section was stored in three matrices: raw Sv data matrix, a binary matrix and a categorical matrix.

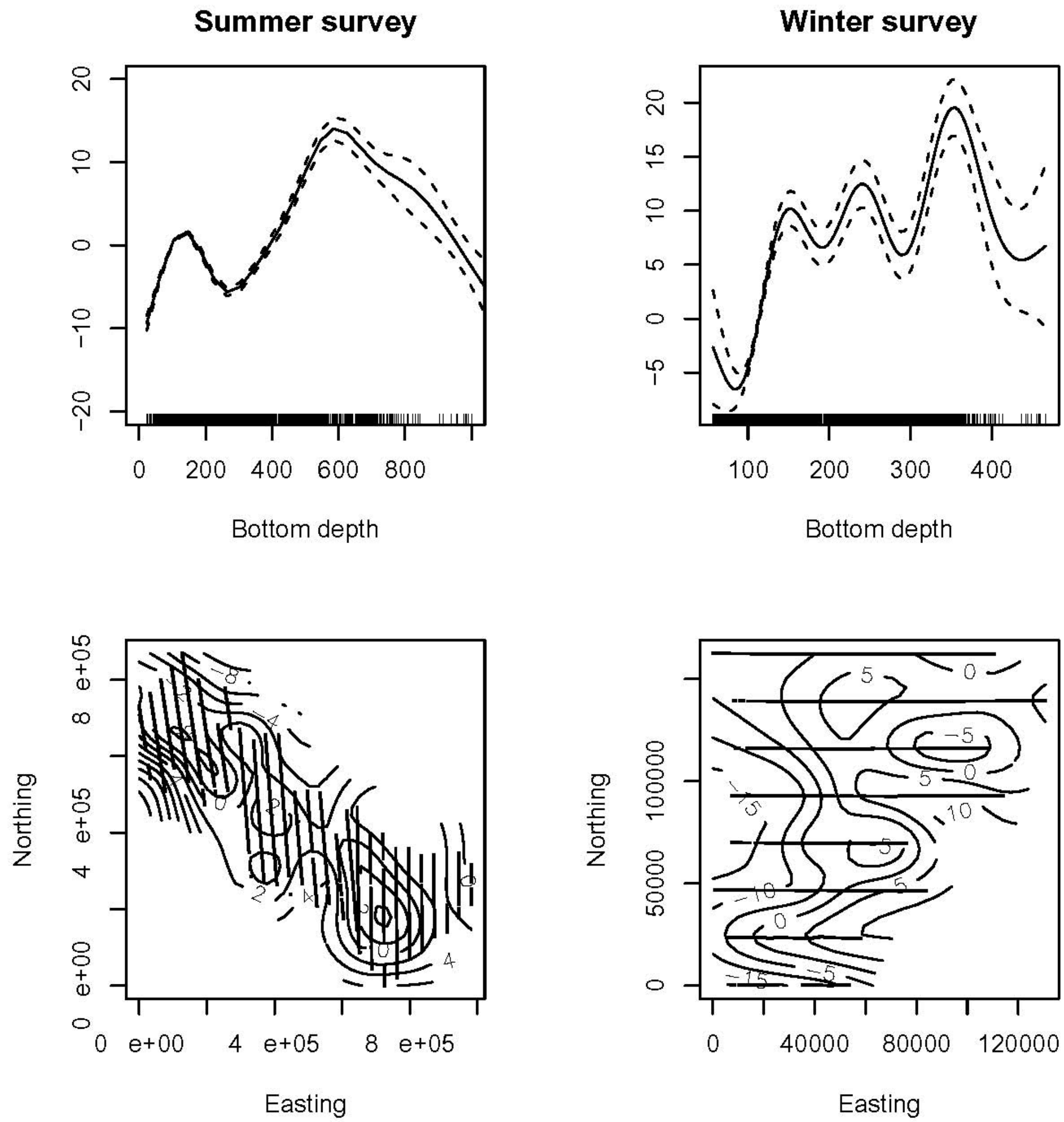

Fig. 5. Results of fitting a GAM on area backscatter coefficient (Sa) data from the summer and winter surveys. Sa was modeled as a function of a one-dimensional smooth curve modeling the relationship with bottom depth, and a two dimensional surface modeling the relationship to location (northing and easting in UTM coordinates).

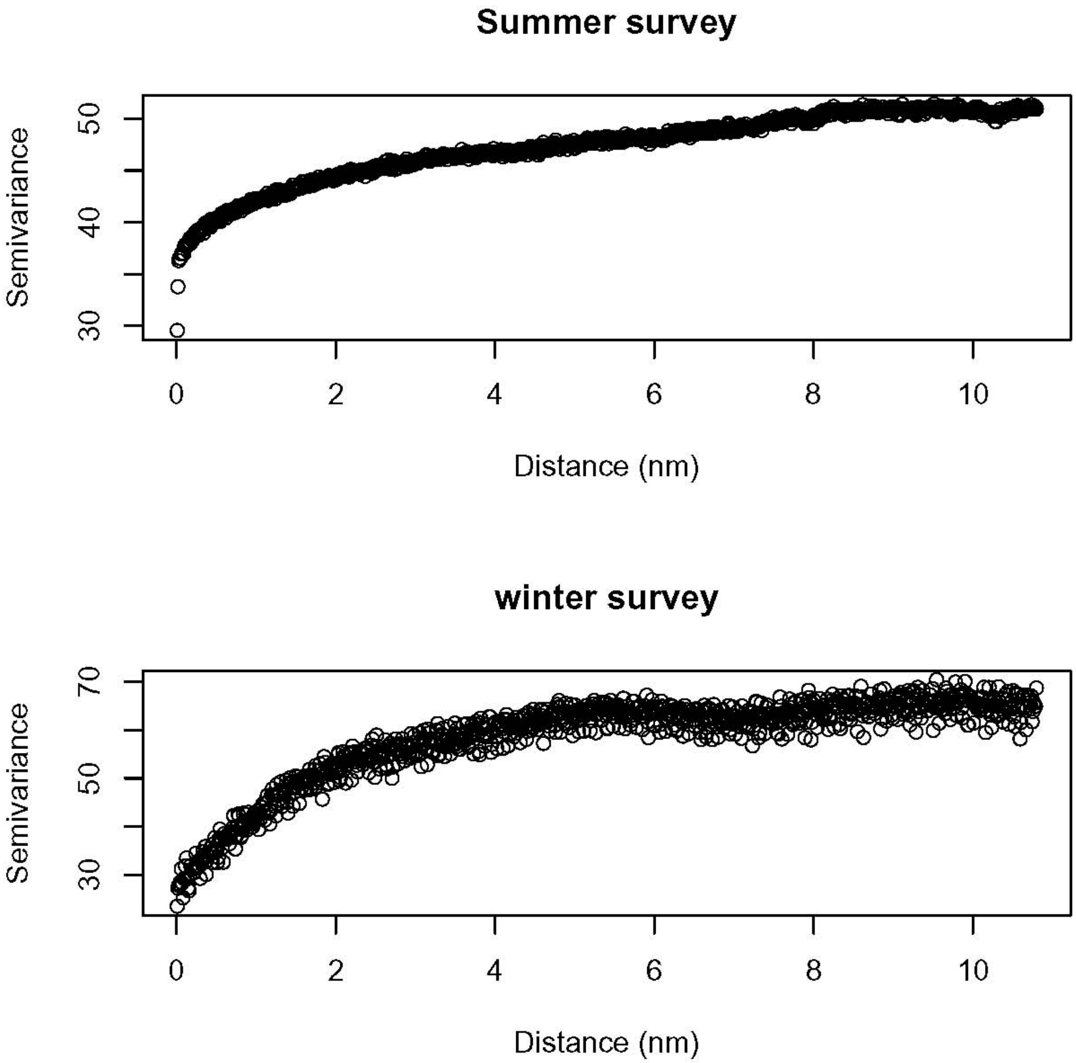

Fig. 6. Empirical semivariograms calculated from residuals of GAMs models.

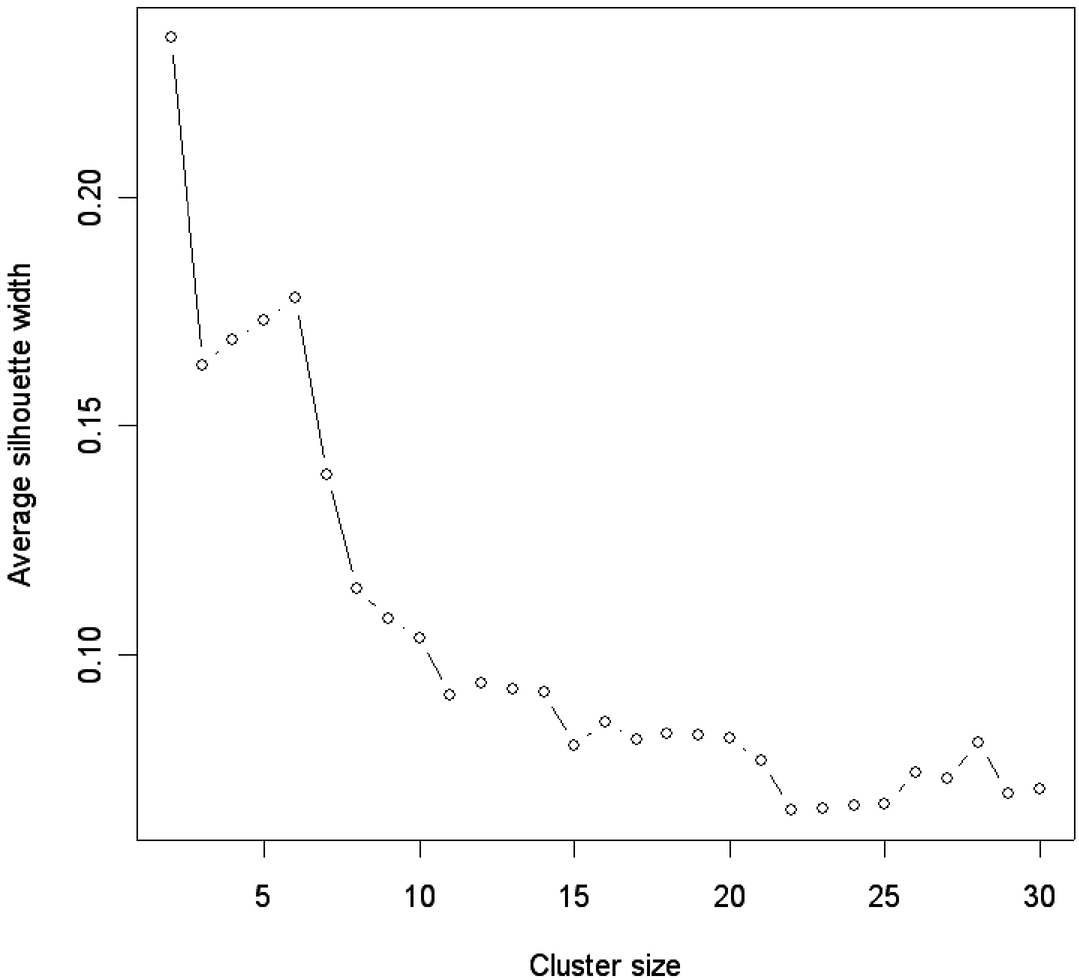

Fig. 7. Average silhouette width of clustering by partition around medoids, for a range of cluster numbers. The average silhouette width is a measure of clustering quality. Results indicate that the optimum number of clusters in the data set is 2, followed by 6.

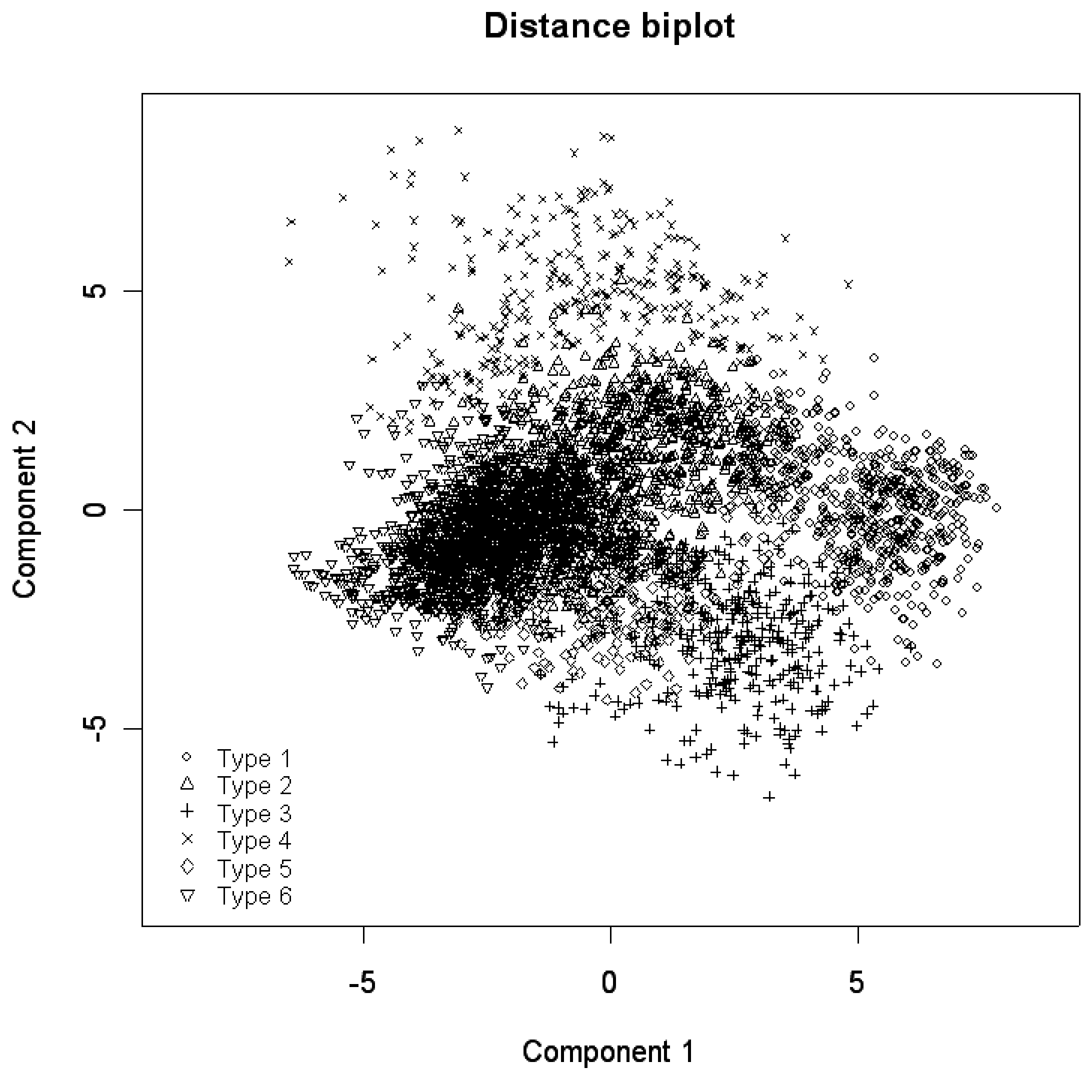

Fig. 8. Location on the reduced space of the two main principal axis of echogram segment classified into six types.

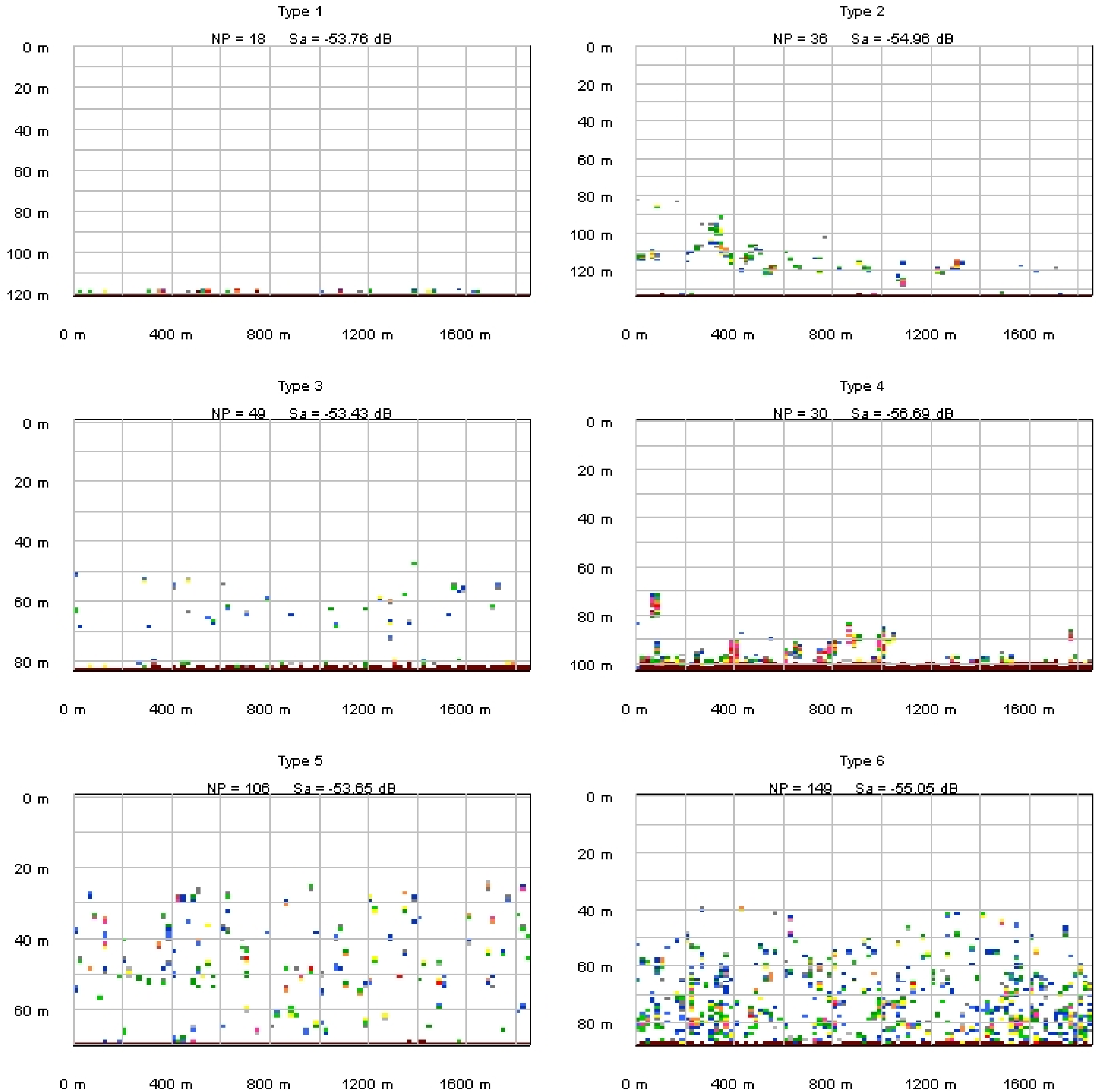

Fig. 9. Representative echogram segments from the six aggregation types, including number of patches (NP) and area backscatter strength (Sa) in each echogram. Segments are 1 nm long. The vertical distance ranges from the surface to the bottom.

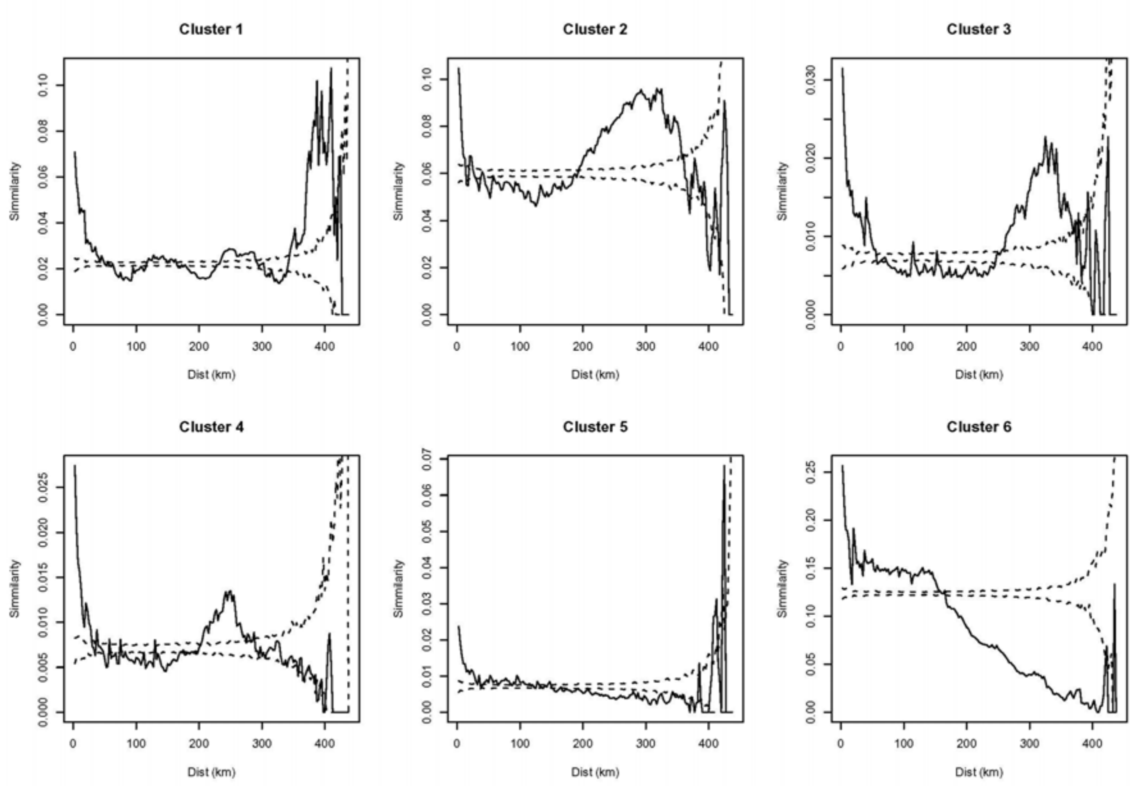

Fig. 10. Modified Ripley's K for the summer survey. Straight lines indicate the proportion of pairs of echogram segments of the same type among all pairs within each distance lag. Dotted lines indicate the 5% and 95% of the similarity indices obtained from 100 random permutations.

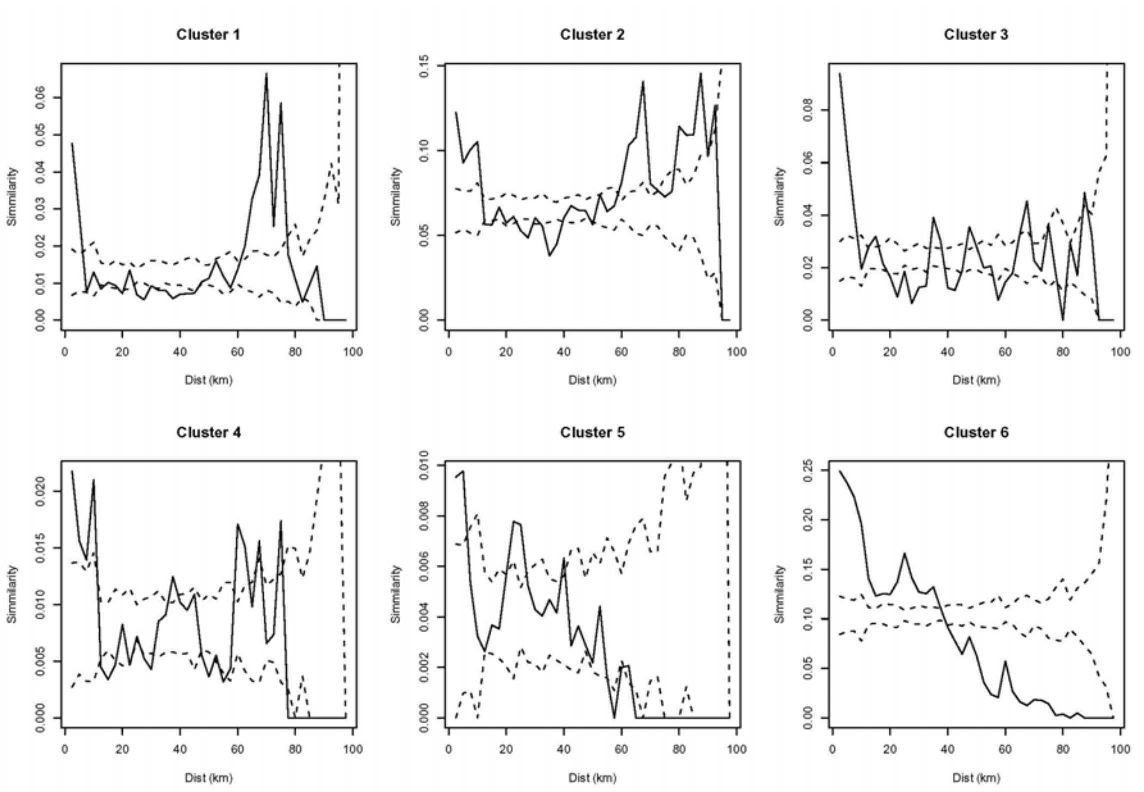

Fig. 11. Modified Ripley's K for the winter survey. Straight lines indicate the proportion of pairs of echogram segments of the same type among all pairs within each distance lag. Dotted lines indicate the 5% and 95% of the similarity indices obtained from 100 random permutations.

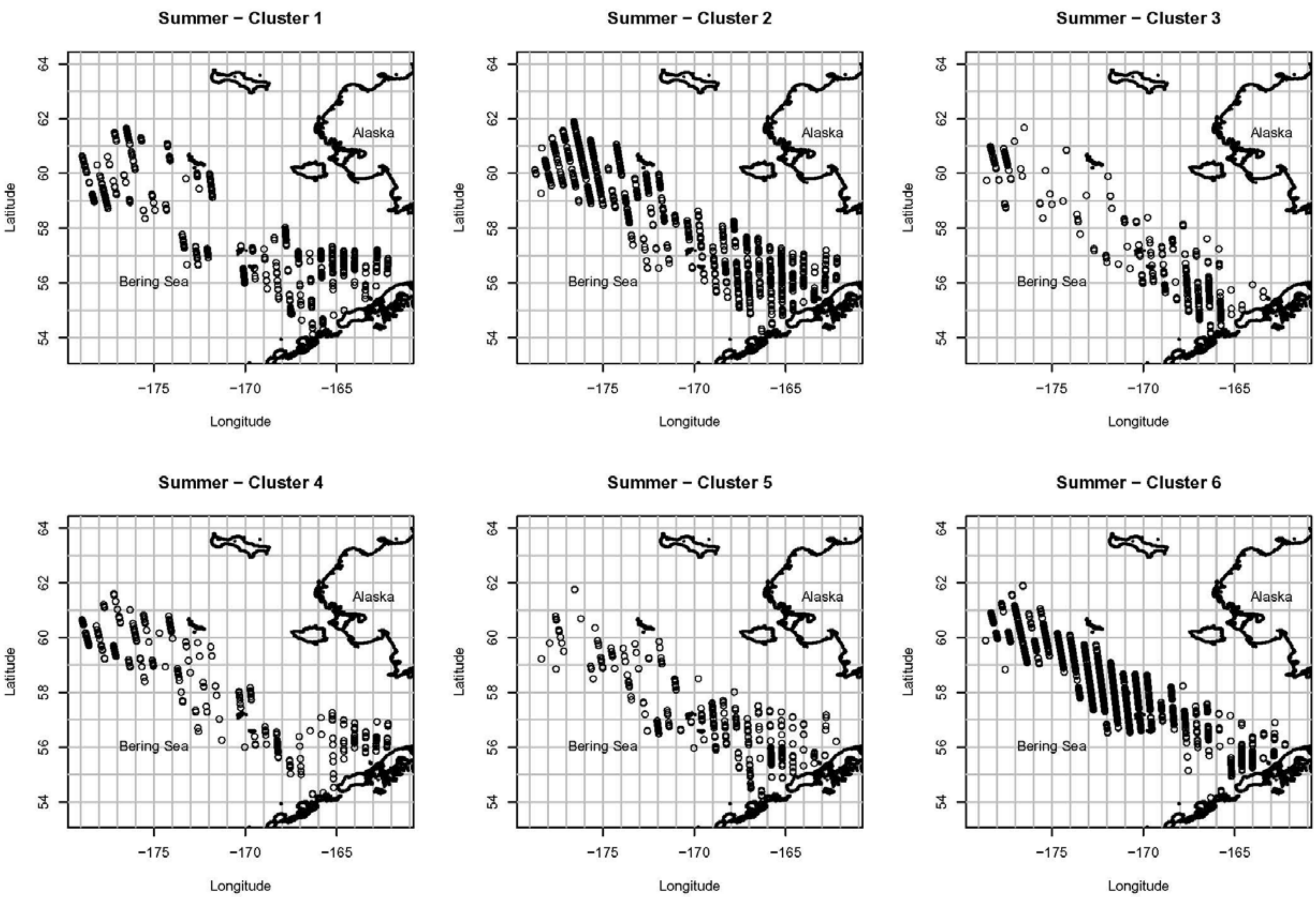

Fig 12. Location of the echogram segments classified into the six echogram types. Data from the summer survey.

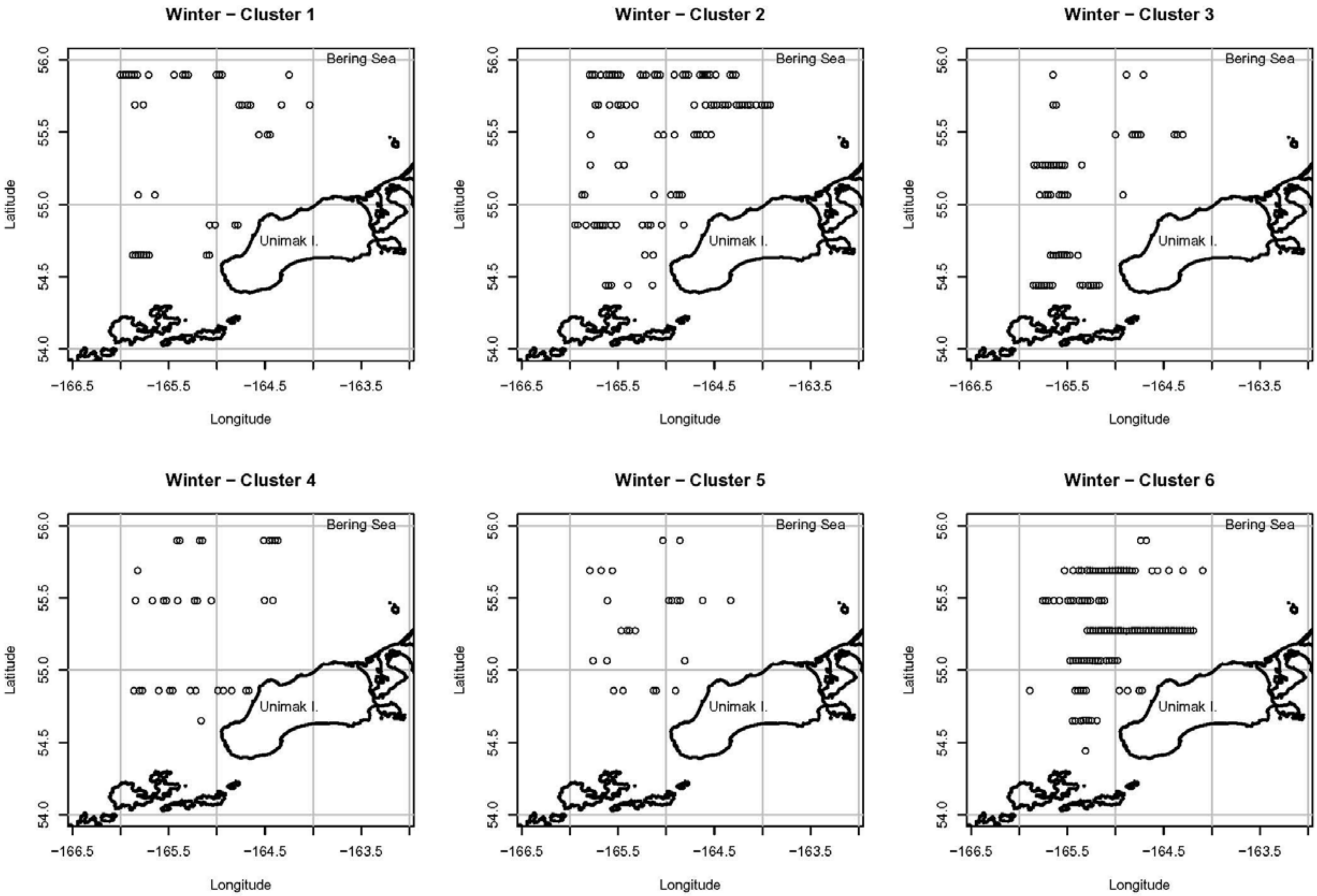

Fig 13. Location of the echogram segments classified into the six echogram types. Data from the winter survey.